IEEE Access
Multidisciplinary | Rapid Review | Open Access Journal

Received January 12, 2020, accepted January 20, 2020, date of publication January 31, 2020, date of current version February 7, 2020.

Digital Object Identifier 10.1109/ACCESS.2020.2970611

An FSS-Backed Reflection/Transmission Reconfigurable Array Antenna

WENTAO LI, (Member, IEEE), YIMING WANG, SHUNLAI SUN, AND XIAOWEI SHI, (Senior Member, IEEE)

Science and Technology on Antenna and Microwave Laboratory, Department of Electronic Engineering, Xidian University, Xi'an 710071, China

Corresponding author: Wentao Li (wtli@mail.xidian.edu.cn)

This work was supported in part by the Shaanxi Natural Science Foundation under Grant 2018JM6049, in part by the Ningbo Natural Science Foundation, in part by the Foundation of Science and Technology on Electromechanical Dynamic Control Laboratory, China, and in part by the National Natural Science Foundation of China under Grant 61571356.

ABSTRACT Reflectarray and transmitarray antennas have been widely used in radar detection systems and satellite communications. Simultaneous realization of reflection and transmission of electromagnetic waves under the same antenna aperture will undoubtedly save more space and cost, which is beneficial to their broader applications. In this paper, an antenna element based on active frequency selective surface (FSS) is proposed, which can realize band-pass and band-stop conversion by controlling the bias of the loaded PIN diode. Then, a reconfigurable antenna array including 9×9 elements and fed through a horn antenna is designed and demonstrated. Simulation and measurement results show that the designed antenna can realize the conversion of reflection and transmission at the frequency of 11 GHz, and the measured peak gain of reflection and transmission reaches 18.2 dBi and 20.9 dBi, respectively.

INDEX TERMS FSS, PIN diodes, reconfigurable, reflectarray, transmitarray.

I. INTRODUCTION

Aperture antenna have long been used to provide the high-gain beam in radar systems. Array lenses (namely, transmitarrays (TA)) and reflectarrays (RA) were first proposed in 1949 and 1963 [1], [2]. However, interest in reflectarrays and transmitarrays did not really begin seriously until planar microstrip antennas were popularized in the 1990s [3]–[8]. The reflectarray and transmitarray antenna integrates the advantages from both microstrip array antenna and parabolic/lens antenna. Compared with traditional aperture antennas, TAs and RAs are the better high-gain antenna alternatives due to their low-profile nature, low weight and ease of manufacture. Compared with the traditional phased array antennas, they can achieve flexible beam scanning without complex phase shift networks and T/R components. Hence, RAs and TAs have a broad application prospect in the fields of space exploration, radar detection and satellite communication [9]-[11].

Recently, researchers have introduced the reconfigurable technique into the design of RAs and TAs, and obtained the reconfigurable reflectarray (RRA) and transmitarray (RTA) antennas. On one hand, discrete components such as PIN diodes, MEMS switches and varactors are used to achieve the tunable electrical properties under the premise that the overall structure and the aperture of the array remain unchanged; on the other hand, some artificial materials such as metamaterial, graphene and liquid crystal are used as the substrate of the array element to achieve the same effect at high frequency [9]. In addition, the frequency selective surface (FSS) is widely used in the design of reconfigurable reflectarrays because it can effectively control the scattering of electromagnetic (EM) waves at certain frequency [12]–[15].

Several reconfigurable techniques for reflectarray and transmitarray antennas have been studied and designed. For example, a circular reflectarray including 244 units was designed in [16], and by controlling the loaded PIN diodes, beam scanning in three angles were achieved. In [17], MEMS technology was used in the design of a 1-bit reflectarray cell to achieve the reconfigurable of dual-linear polarization. In [18] and [19], reconfigurable reflectarray antennas with 16×16 elements were demonstrated, which employed liquid crystals as the substrate and operated at millimeter-wave frequencies. However, most of antenna designs mentioned above are basically simplex despite the reconfigurable reflectarray and transmitarray antennas have made considerable

The associate editor coordinating the review of this manuscript and approving it for publication was Giorgio Montisci.

progress in the past few years. Of course, relevant studies on dual-mode reflection/transmission array antenna have also been proposed recently. In 2015, a dual-mode plasma reflectarray/transmitarray antenna was designed in [20] and [21]. By controlling the ionized plasma gas density of the square ground plane, two modes of operations were obtained for the same unit cell. In [22], a 1-bit bidirectional reconfigurable transmit-reflect-array was proposed, in which the bidirectional radiation was achieved by utilizing the continuity of the cross-polarized electric field on the surface. In [23], an FSS-backed phase shifting surface array antenna with multimode operation was designed, which was capable of simultaneously exhibiting the functionalities of a transmitarray and a reflectarray at different frequencies. In [24], a novel polarization-dependent R/T amplitude code was proposed which enabled a full-space communication system and larger information capacity. However, how to achieve the dual-mode reflection/transmission array antenna at the same frequency remains to be explored.

In this paper, an FSS with cross structure is designed to achieve the conversion from reflection to transmission by adjusting the state of two PIN diodes. On this basis, a new FSS-backed multi-functional reflection/transmission reconfigurable antenna including 9×9 units is studied and designed, which uses a four-layer substrate structure. By adding reconfigurable FSS bottom layer, the proposed antenna achieves flexible conversion between reflectarray and transmitarray. Compared with the previous studies, the superiority of the proposed antenna array in this paper lies in its ability of transmission/reflection reconfigurable, which switches from a reflectarray to a transmitarray at the same frequency. The measured results agree well with the simulation results.

This paper is organized as follows: Section II introduces the specific structure of the designed FSS and analyzes the effect of the state of PIN diode on the scattering characteristics of the FSS. In section III, the reflection/transmission reconfigurable antenna is designed and fabricated, and the results of simulation and measurement are compared. Finally, conclusions are drawn in section IV.

II. DESIGN AND SIMULATIONS OF PATCH ELEMENTS

The metal ground of the reflectarray antenna is usually fully covered, and it has the effect of perfect reflection so that the influence of the reflection coefficient can be completely ignored in the design of reflection element. However, in the transmitarray antenna design, the magnitude and phase range of the transmission coefficient must be taken into account. FSS has frequency selectivity and can show certain property (reflection or transmission) at a certain frequency. To realize the reflectarray, the FSS is employed as a ground of the array element to completely reflect the incident wave at a certain frequency. Nevertheless, the FSS can also act as a good candidate for realizing the transmitarray, since it exhibits good transmission performance and can make the incident wave pass through the transmission surface with minimum loss.

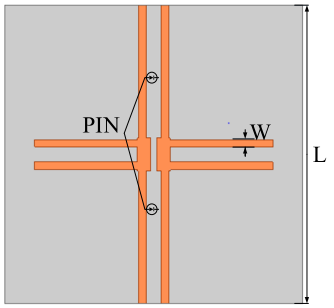

FIGURE 1. FSS structure.

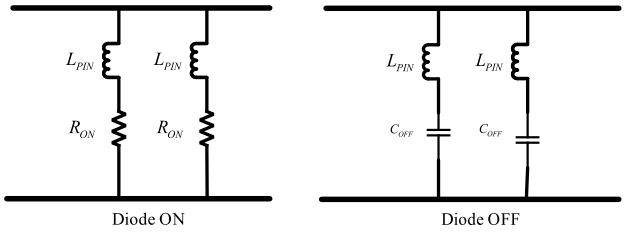

FIGURE 2. The EC of the FSS (a) Diode state: ON (b) Diode state: OFF.

In this work, the structure of the FSS is carefully selected to avoid inherent capacitance in the FSS given that all the adjacent FSS are connected to each other, as illustrated in Fig. 1. The employed FSS has a cross architecture, and four rectangular slots with the same width are separated on the four branch arms. The cross structure is divided into left and right parts by two PIN diodes, the two PIN diodes are oriented in the same ways and work in the same states given a positive or negative biasing voltage and the resonance structure of the FSS is changed by the state of the two PIN diodes. The size of the FSS is determined as $L = 20$mm and $W = 0.5$mm, and the Rogers 4350B ($\varepsilon_r = 3.66$, $\tan\delta = 0.004$) is selected as the substrate of the element.

The function of the FSS mechanism can be explained by an equivalent circuit (EC) model in Fig. 2. The diodes (PHILIPS BAP70-03) are modeled in accordance with [25], where $R_{ON} = 1.5\,\Omega$, $C_{OFF} = 0.1$pF, and $L_{PIN} = 1.5$nH. When the diode is turned on, as shown in Fig. 2 (a), the EC of the FSS fails to resonate due to the lack of capacitance. In this state the FSS can exhibit transmission performance and allow most of the energy to pass through. As shown in Fig. 3(a), at the frequency of 11 GHz, the reflection coefficient is lower than -20 dB and the transmission coefficient is larger than -1 dB. When the diode is disconnected, as displayed in Fig. 2 (b), the EC is equivalent to the traditional parallel LC resonate circuit. It provides a very high impedance and completely reflects the EM wave at the resonance frequency. As shown in Fig. 3 (b), at the frequency of 11 GHz, the transmission coefficient is lower than -20 dB and the reflection coefficient is larger than -1 dB in the simulation. Therefore, by adding PIN diode, this designed FSS structure can be flexibly converted from transmission to reflection by switching the state

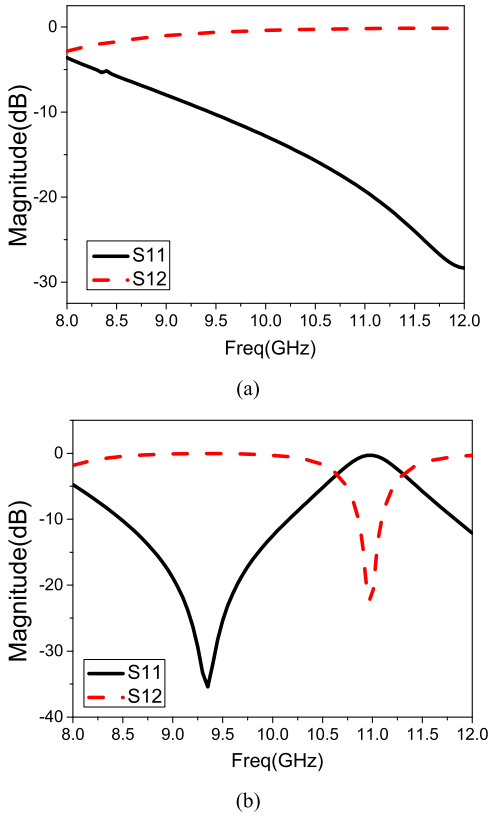

FIGURE 3. The scattering parameters of the FSS: (a) Diode state: ON (b) Diode state: OFF.

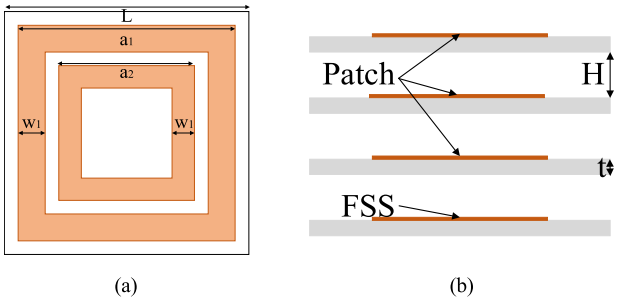

FIGURE 4. Structure of the proposed element: (a) Top view (b) Side view.

of the PIN diode from ON to OFF, which has a broad application prospects.

For the proposed reconfigurable antenna array, the geometry of the array element is shown in Fig. 4. The unit adopts a four-layer patch structure, and these layers are respectively printed on four dielectric substrates with the same air gaps (H). The FSS structure is etched on the surface of the underlying dielectric substrates while the radiation patch, a concentric double square rings structure, is printed on the surface of the upper three substrates. The phase shift of the element can be controlled by adjusting the length of the outer ring ($a1$). The width of the inner and outer rings is $w1$, and the length of the inner ring is $a2$. Furthermore, $a1 = k \times a2$, where k is a proportional value.

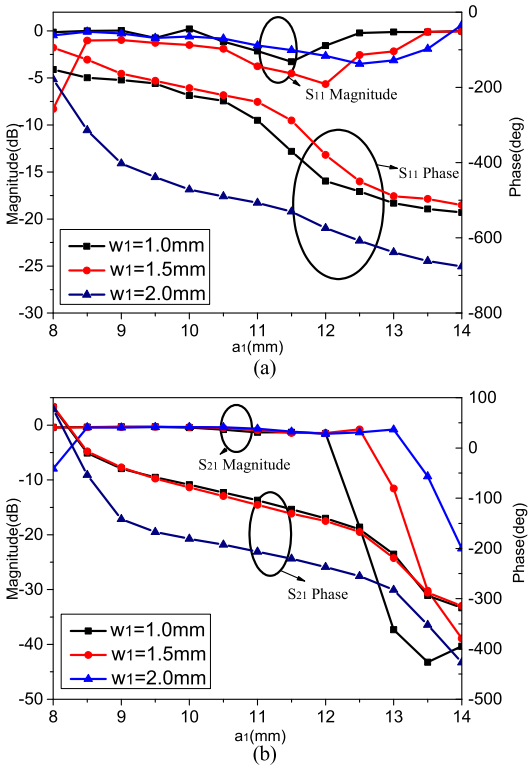

FIGURE 5. Effect of square ring width ($w1$) on scattering parameters and phase of the element. (a) Diode OFF (b) Diode ON.

In designing a reflection/transmission reconfigurable array antenna, the magnitudes of the scattering parameters of the element have to be considered since they greatly affect the performance of the reflectarray and transmitarray. Note that, on the premise of phase compensation, the reflection and transmission phase curves should first cover an angle range of almost 360° under the same abscissa. Besides, the reflection and transmission phase curves should be approximately parallel, so as to ensure that the array with phase compensation has the same beam direction in different operating modes. To satisfy the above requirements, the performance of the proposed element is simulated and its structural parameters are optimized through HFSS.

From the perspective of theoretical design, the structure and size of the radiating element, the material and thickness of the substrate, the number of layers of the element, and the thickness of the air between each element layer can all affect the reflection and transmission phases. In this paper, the substrate material and the basic structure of the radiating element are determined first, then only the width and size of the rings are the variables related to the radiating element. In addition, since the phase is compensated by changing the size of the rings, the size proportional coefficient of the inner and outer rings is selected as the other variable. In this way, the final variables to be optimized are determined, namely, the size proportional coefficient of the inner and outer rings (k), the width of the rings ($w1$), the number of element layers and the thickness of the air layer (H). After that,

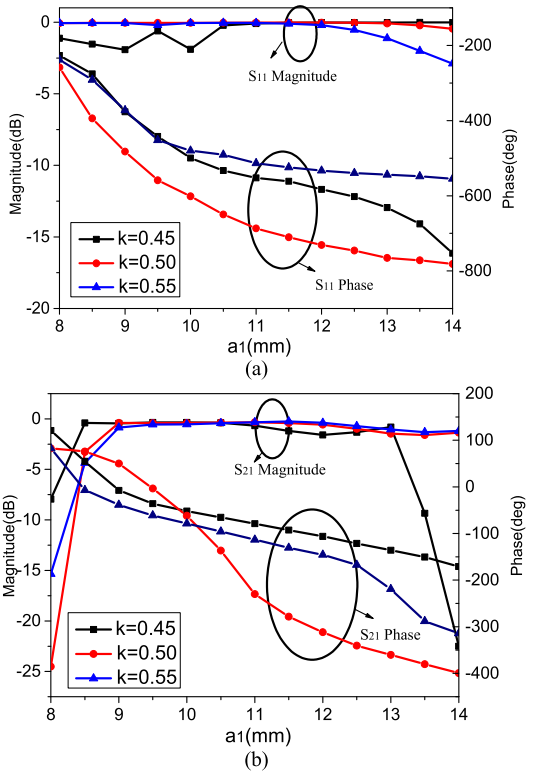

FIGURE 6. Effect of the size ratio of inner and outer rings (k) on scattering parameters and phase of the element. (a) Diode OFF (b) Diode ON.

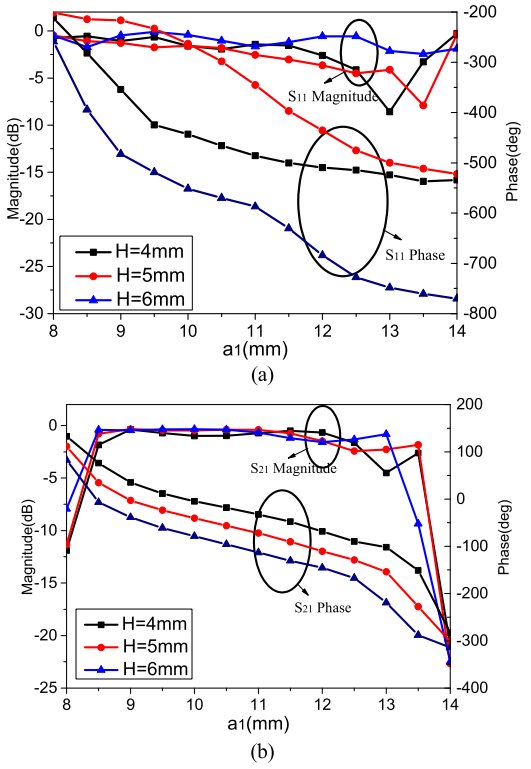

FIGURE 7. Effect of the air layer thickness (H) on scattering parameters and phase of the element. (a) Diode OFF (b) Diode ON.

the parameters of each variable are scanned in turn while the other variables are kept unchanged. The results of each variable are obtained by comparing the compensation range and approximate degree of the reflection/transmission phase. Finally, the structure size of the whole element is determined.

Fig. 5 (a) presents the simulated reflection coefficient and phase versus $a1$ for different $w1$ when the PIN diode is in the OFF state at 11 GHz. The range of the reflection phase changes, and the less than -1 dB coverage range of the reflection coefficient is the largest when the width of the inner and outer rings is 2 mm. Fig. 5 (b) depicts the variations of transmission coefficient and phase with $a1$ for different $w1$ when the state of PIN diode is ON. With the increase of $w1$, the transmission bandwidth increases, and the transmission phase is consistent with the reflection phase when $w1 = 2$mm. Figs. 6 (a) and (b) depict the simulated reflection/transmission coefficient and phase for different k and PIN diode states as a function of $a1$ at 11 GHz, respectively. The reflection and transmission phases are the same when$k = 0.5$mm, and the reflection/transmission coefficient remains unchanged for different values of k. Figs. 7 (a) and (b) demonstrate that the change in the value of H influences the reflection coefficient and phase while slightly affecting the transmission coefficient and phase. The dielectric substrate interval is selected to be $H = 6$mm to ensure the transmission phase consistent with the reflection phase. Figs. 8 (a) and (b) display the reflection/transmission coefficient and phase versus $a1$ for different layers and states of the PIN diodes at 11 GHz, respectively. Notably, with the increased number of layers of a dielectric structure, the range of reflection/transmission phase and the coverage range of reflection/transmission coefficient less than -1 dB also increase. To keep the transmission phase consistent with the reflection phase, a four-layer dielectric substrate structure is finally adopted in accordance with the simulation results.

With all the selected parameters, the optimized reflection and transmission phases of the element are shown in Fig. 9. It can be seen that the compensation ranges of reflection and transmission phases of the element exceed 360°, and the two phase curves are approximately parallel, which can satisfy the design requirements of reflection and transmission array.

III. ARRAY ANTENNA DESIGN AND REALIZATION

By compensating the phase of each element, it is easily to control the beam to the desired direction. Since the array antenna to be designed in this paper has no need of beam deflection, the phase of compensation for the array element is only related to the position of the array element relative to the center of the aperture. Thus, we have

$$\phi_R(x_i, y_i) = k_0 d_i \tag{1}$$

where $\phi_{R(xi,yi)}$ represents the phase to be compensated, $k0$ is the propagation constant of electromagnetic wave in free space, d_i denotes the distance from the feed antenna to the unit. Assuming the coordinates of the feed antenna are

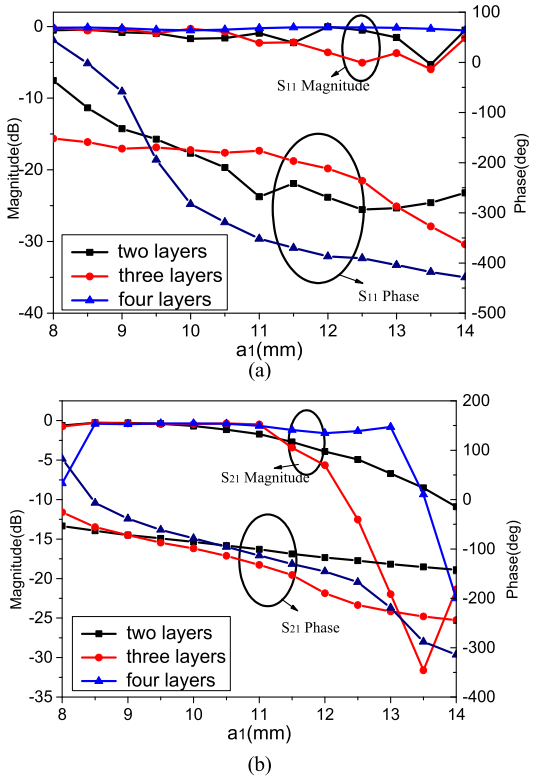

FIGURE 8. Effect of the number of radiating element layers on scattering parameters and phase of the element. (a) Diode OFF (b) Diode ON.

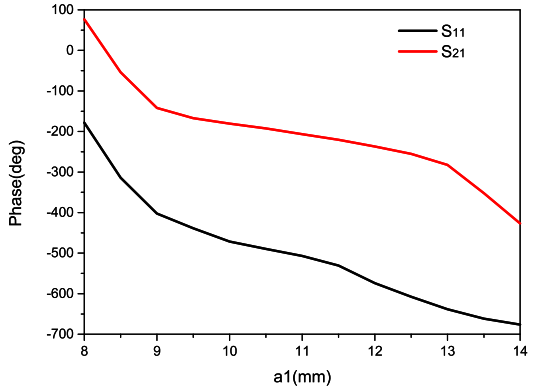

FIGURE 9. Reflection/transmission phase of the optimized antenna element.

(xf, yf, zf), we have:

$$d_i = \sqrt{\left(x_i - x_f\right)^2 + \left(y_i - y_f\right)^2 + z_f^2} \tag{2}$$

In Section II, a reconfigurable element is designed with high transmission and reflection conversion capability at 11 GHz. Hence, this reflection/transmission reconfigurable array antenna can be easily realized by using the designed element. To design reconfigurable array antennas, the arrangement and phase distribution of the FSS-backed elements cannot be changed. Thus, flexible conversion between the reflectarray and the transmitarray can be realized by controlling the switching states on the FSS.

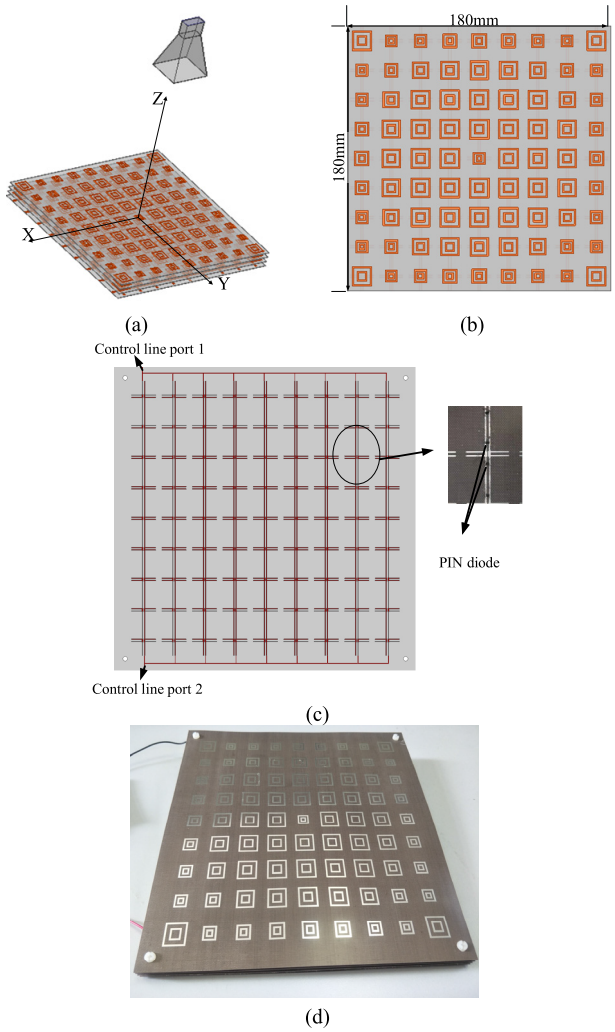

FIGURE 10. Structure of the reflection/transmission reconfigurable antenna array. (a) Whole antenna structure, (b) Designed antenna layout, (c) FSS layer with control lines and (d) Assembled antenna.

Figs. 10 (a) and (b) show the 3-D view of the reflection/transmission reconfigurable array antenna and the distribution of the elements in the plane, respectively. As can be seen, the antenna array adopts a multi-layer square structure, in which 9×9 elements are arranged in the xoy-plane. The upper three layers of dielectric substrates are printed with the same patches, and the FSS is periodically arranged on the bottom dielectric substrates. The overall aperture of the antenna array is 180 mm $\times$ 180mm. A horn antenna is selected as the feed, which is placed at the height of 180mm (focal-diameter ratio F/D $=$ 1). The phase distribution of each element is calculated by MATLAB. The reflection/transmission reconfigurable array antenna is fabricated. Fig. 10 (c) shows the FSS layer with control lines, notably, due to the PIN diodes the array adopts have the same working status and the longer arm of the FSS is the head-tail, two control lines are drawn directly from the left and right sides of the longer arm of the FSS. Then the control lines connecting the different pins of the diodes are respectively concentrated on the two sides of the FSS layer. When the two sides are connected to the

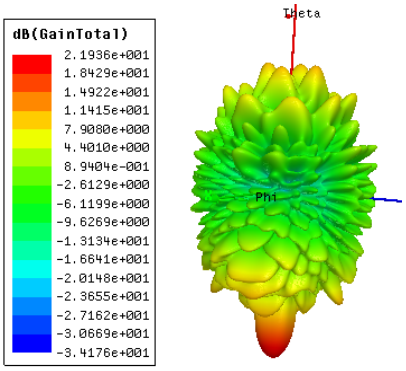

(a)

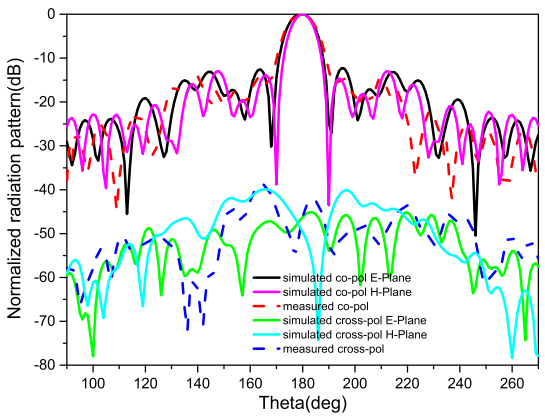

(b)

FIGURE 11. (a) Simulated 3-D radiation pattern of the designed array. (b) Simulated and measured 2-D radiation patterns of the designed transmitarray.

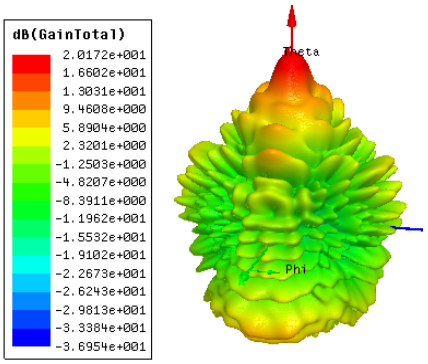

(a)

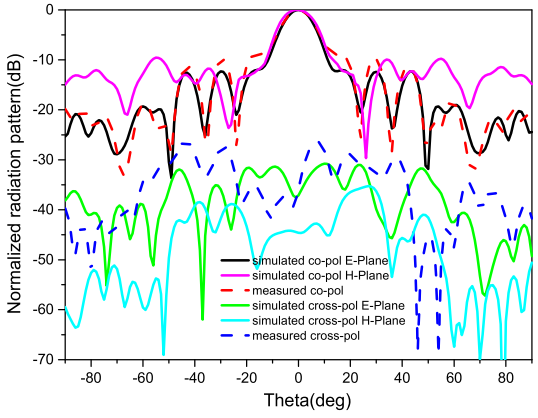

(b)

FIGURE 12. (a) Simulated 3-D radiation patterns of the designed array. (b) Simulated and measured 2-D radiation patterns of the designed reflectarray.

positive and negative poles of the bias voltage respectively, all of the diodes can be controlled. The specific physical photograph is shown in Fig. 10 (d).

The antenna acts as a transmitarray when the diode is in the ON state. That is, the incident wave from the feed antenna passes through the transmission front, and then is compensated by the transmission unit to form a high gain beam with a specific direction on the other side of the front. Fig. 11 shows the 3-D and the 2-D transmission patterns at 11 GHz. It displays that the direction of the transmitted beam is perpendicular to the transmission plane. The results indicate that the maximum simulation gain of the antenna is 21.9 dBi, and the measured gain is 20.9 dBi. The cross-polarization levels of the simulated and measured results are all below -40 dB, and the half-power beam width (HPBW) of the transmitarray is 12°. The first side lobe level (SLL) of the transmitarray are -13 dB and -14 dB, respectively. Thus, a favorable agreement is achieved between the simulated and the measured results.

The antenna can be transformed into a reflectarray without changing the overall structure, aperture size, and compensation phase of the element, simply by keeping the diode off. That is, the incident wave from the feed antenna is totally reflected by the reflecting front, forming a high gain beam with a specific direction at the aperture of the front. Fig. 12 presents the 3-D and the 2-D reflection patterns of the reflectarray when the diode is in the OFF state at 11 GHz, respectively. It can be discovered that the reflected beam along the $+Z$-axis is perpendicular to the reflection plane. The results show that the maximum simulation gain of the antenna is 20.1 dBi, and the measured gain is 18.2 dBi. The cross-polarization levels of the simulated and measured results are all below -30 dB, and the half-power beam width (HPBW) of the transmitarray is 12°. The first SLL for the reflectarray are -13 dB and -7 dB, respectively.

Table 1 summarizes the simulation and test results for the reflectarray and transmitarray antenna in details. When the array antenna acts as a transmitarray, the simulation and test results have nearly the same HPBW when working at 11 GHz. The first SLL is approximately 1 dB higher in the simulation result than that in the test results. Besides the gain is slightly higher in the simulation than that in the test. On the other hand, when the array antenna acts as a reflectarray, we find the simulation and test results have the same HPBW when working at 11 GHz. The simulation gain is approximately 2 dB higher than the test one, and the measured SLL is 6 dB higher than the simulated result. This is mainly caused by that the main lobe of the radiation pattern has a certain

TABLE 1. Simulation and Test Results of Reflectarray and Transmitarray.

Simulation/test	Transmitarray	Reflectarray
PIN diode operation	ON	OFF
Working frequency	11 GHz	11 GHz
Gain (dBi) (Sim./Mea.)	21.9/20.9	20.1/18.2
Beam pointing	$-z$	$+z$
(HPBW)	12°/12°	12°/12°
SLL (dB) (Sim./Mea.)	−13/−14	−13/−7
Efficiency(%)	79.4	64.6

degree of expansion, and this phenomenon is a bit obvious in the measured results. The main reason for the expansion of the main lobe is probably attributed to the feed antenna is directly above the array, and the shielding effect has an influence on the radiation of the antenna. The reason why this phenomenon becomes more obvious in the measured results is that, the actual size of the feed antenna used is a bit larger than that in the simulation, thus causing a bit larger shielding effect of the feed antenna than that in simulation. Except the rise of the sidelobe, it can be discovered that the simulation results are in good agreement with the test results, Moreover, a flexible conversion between the reflectarray antenna and the transmitarray antenna is verified by simply adjusting the ON/OFF state of the PIN diode.

IV. CONCLUSION

In this study, a reflection/transmission reconfigurable array antenna based on FSS-back element has been designed and implemented. The superiority of the proposed antenna array design lies in its reconfigurable performance of the transmission/reflection, which can be dynamically converted between the reflectarray and transmitarray antennas at 11 GHz, by controlling the ON/OFF state of the PIN diode. More importantly, the transmitarray can be transformed into a reflectarray without changing the overall structure, aperture size, and compensation phase of the element, but only by changing the ON state of the diode to the OFF state. By comparing the results of simulation and measurement, it is found that the results of the antenna under two conditions agree well and both of the reflectarray and the transmitarray get good performance. These results validate that the designed array antenna has flexible reconfigurable performance and broad application prospects.

REFERENCES

[1] W. Kock, "Path-length microwave lenses," *Proc. IRE*, vol. 37, no. 8, pp. 852–855, Aug. 1949.
[2] D. Berry, R. Malech, and W. Kennedy, "The reflectarray antenna," *IEEE Trans. Antennas Propag.*, vol. 11, no. 6, pp. 645–651, Nov. 1963.
[3] J. Huang, "Microstrip reflectarray," in *Antennas Propag. Soc. Symp. Dig.*, vol. 2, Dec. 2002, pp. 612–615.
[4] D. Pozar, "Reviews and Abstracts [review of 'Reflectarray antennas (Huang, J. and Encinar, J.A.; 2008)]," *IEEE Antennas Propag. Mag.*, vol. 50, no. 6, pp. 127–129, Dec. 2008.
[5] J. Ginn, B. Lail, and G. Boreman, "Sub-millimeter and infrared reflectarray," U.S Patent 7 623 071 B2, Nov. 24, 2009.
[6] H. F. Ma and T. J. Cui, "Three-dimensional broadband and broad-angle transformation-optics lens," *Nature Commun.*, vol. 1, no. 8, p. 124, Nov. 2010.
[7] X. Yang, S. Xu, F. Yang, M. Li, Y. Hou, S. Jiang, and L. Liu, "A broadband high-efficiency reconfigurable reflectarray antenna using mechanically rotational elements," *IEEE Trans. Antennas Propag.*, vol. 65, no. 8, pp. 3959–3966, Aug. 2017.
[8] J. Ginn, B. Lail, J. Alda, and G. Boreman, "Planar infrared binary phase reflectarray," *Opt. Lett.*, vol. 33, no. 8, pp. 779–781, Apr. 2008.
[9] S. V. Hum and J. Perruisseau-Carrier, "Reconfigurable reflectarrays and array lenses for dynamic antenna beam control: A review," *IEEE Trans. Antennas Propag.*, vol. 62, no. 1, pp. 183–198, Jan. 2014.
[10] S. Montori, F. Cacciamani, R. V. Gatti, R. Sorrentino, G. Arista, C. Tienda, J. A. Encinar, and G. Toso, "A transportable reflectarray antenna for satellite ku-band emergency communications," *IEEE Trans. Antennas Propag.*, vol. 63, no. 4, pp. 1393–1407, Apr. 2015.
[11] P. Nayeri, F. Yang, and A. Elsherbeni, "Beam scanning reflectarray antennas: A technical overview and state of the art," *IEEE Antennas Propag. Mag.*, vol. 57, no. 4, pp. 32–47, Aug. 2015.
[12] Q. Chen, L. Chen, Y. Fu, L. Liu, and J. Bai, "Absorptive frequency selective surface using parallel LC resonance," *Electron. Lett.*, vol. 52, no. 6, pp. 418–419, Mar. 2016.
[13] Q. Chen, S. Yang, J. Bai, and Y. Fu, "Design of absorptive/transmissive frequency-selective surface based on parallel resonance," *IEEE Trans. Antennas Propag.*, vol. 65, no. 9, pp. 4897–4902, Sep. 2017.
[14] K. Zhang, W. Jiang, and S. Gong, "Design bandpass frequency selective surface absorber using LC resonators," *IEEE Antennas Wireless Propag. Lett.*, vol. 16, pp. 2586–2589, 2017.
[15] H. Huang and Z. Shen, "Absorptive frequency-selective transmission structure with square-loop hybrid resonator," *IEEE Antennas Wireless Propag. Lett.*, vol. 16, pp. 3212–3215, 2017.
[16] E. Carrasco, M. Barba, and J. A. Encinar, "X-band reflectarray antenna with switching-beam using PIN diodes and gathered elements," *IEEE Trans. Antennas Propag.*, vol. 60, no. 12, pp. 5700–5708, Dec. 2012.
[17] T. Debogovic and J. Perruisseau-Carrier, "Low loss MEMS reconfigurable 1-bit reflectarray cell with dual-linear polarization," *IEEE Trans. Antennas Propag.*, vol. 62, no. 10, pp. 5055–5060, Oct. 2014.
[18] A. Moessinger, R. Marin, S. Mueller, J. Freese, and R. Jakoby, "Electronically reconfigurable reflectarrays with nematic liquid crystals," *Electron. Lett.*, vol. 42, no. 16, pp. 899–900, 2006.
[19] S. Bildik, S. Dieter, C. Fritzsch, W. Menzel, and R. Jakoby, "Reconfigurable folded reflectarray antenna based upon liquid crystal technology," *IEEE Trans. Antennas Propag.*, vol. 63, no. 1, pp. 122–132, Jan. 2015.
[20] H. A. Malhat, M. M. Badawy, S. H. Zainud-Deen, and K. H. Awadalla, "Dual-mode plasma reflectarray/transmitarray antennas," *IEEE Trans. Plasma Sci.*, vol. 43, no. 10, pp. 3582–3589, Oct. 2015.
[21] H. A. Malhat, M. M. Badawy, S. H. Zainud-Deen, and K. H. Awadalla, "Plasma reflectarray/transmitarray antennas using a single structure," *Plasmonics*, vol. 10, no. 6, pp. 1479–1487, Dec. 2015.
[22] M. Wang, S. Xu, F. Yang, and M. Li, "A 1-bit bidirectional reconfigurable transmit-reflect-array using a single-layer slot element with PIN diodes," *IEEE Trans. Antennas Propag.*, vol. 67, no. 9, pp. 6205–6210, Sep. 2019.
[23] X. Zhong, H.-X. Xu, L. Chen, W. Li, H. Wang, and X. W. Shi, "An FSS-backed broadband phase-shifting surface array with multimode operation," *IEEE Trans. Antennas Propag.*, vol. 67, no. 9, pp. 5974–5989, Sep. 2019.
[24] R. Y. Wu, L. Zhang, L. Bao, L. W. Wu, Q. Ma, G. D. Bai, H. T. Wu, and T. J. Cui, "Digital metasurface with phase code and reflection–transmission amplitude code for flexible full-space electromagnetic manipulations," *Adv. Opt. Mater.*, vol. 7, no. 8, Apr. 2019, Art. no. 1801429.
[25] NXP Semiconductors, Silicon PIN Diode, BAP70-03 Datasheet, Mar. 2014. Accessed: May 2018. [Online]. Available: http://www.nxp.com/documents/data_sheet/BAP70-03.pdf

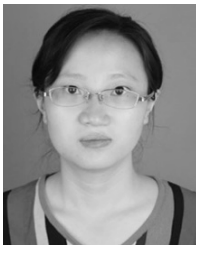

WENTAO LI (Member, IEEE) was born in Shaanxi, China. She received the B.E. degree in electromagnetic engineering and the Ph.D. degree in electromagnetic fields and microwave technology from Xidian University, Xi'an, China, in 2006 and 2010, respectively. She was a Visiting Scholar with The University of Texas at Austin, from August 2015 to August 2016. She is currently an Associate Professor with the School of Electronic Engineering, Xidian University. Her research interests include evolutionary optimization techniques, antenna arrays, and MIMO antennas.

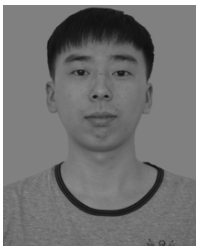

YIMING WANG was born in Shandong, China, in 1996. He received the B.E. degree in electronic information engineering from Xidian University, Xi'an, China, in 2018, where he is currently pursuing the master's degree in electromagnetic fields and microwave technology with the Science and Technology on Antenna and Microwave Laboratory. His research interests include reconfigurable antenna design, antenna arrays, and optimization technology.

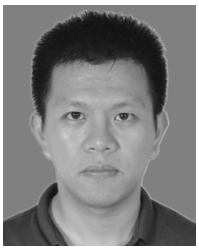

SHUNLAI SUN was born in Hunan, China, in 1993. He received the B.E. degree in electronic information engineering and the master's degree in electronics and communication engineering from Xidian University, Xi'an, China, in 2016 and 2019, respectively. His research interests include phase shifting surface array antennas and reconfigurable antenna design.

XIAOWEI SHI (Senior Member, IEEE) was born in Guangdong, China, in 1963. He received the B.S. degree in radio physics, the M.Eng. degree in electrical engineering, and the Ph.D. degree in electromagnetic field and microwave technology from Xidian University, Xi'an, China, in 1982, 1990, and 1995, respectively. From 1996 to 1997, he was a Cooperator of a Postdoctoral research work with the Electronics and Telecommunications Research Institute, South Korea. He has been a Professor and an Advisor of Ph.D. degree students with Xidian University. In recent years, he mainly studies smart antennas. His research interests include the theory of microwave networks, microwave measurement, and electromagnetic inverse scattering, and the theory of electromagnetic variation, electromagnetic compatibility, and smart antennas.